OPEN ACCESS

STUDY ON EROSION FAILURE MECHANISM OF HIGH-PRESSURE FRACTURING PUMP KEY STRUCTURES

Xin Huang[1,], Jiankang Chen[1], Zhongliang Wang[2], Feng Wang[3]*
[1]School of Engineering, Tongren Polytechnic College，Tong Ren,554300, China;
[2]Petrochina Changqing oil field Company first gas production plant，Xi An 710000, China;
[3]NO.3 Drilling Engineering Company,BHDC, CNPC,Tianjing,300280

Abstract - In order to study the erosion failure mechanism of valve and valve seat of five-cylinder plunger pump, and according to the hydraulic end structure of the five-cylinder plunger pump and Adolf's differential equation of motion, the three dimension transient flow field models under different impulses are established based on the computational fluid dynamics theory. A qualitative and quantitative analysis of the flow field of a periodic plunger pump is carried out. The results show that the velocity of fluid passing through the valve clearance of the pump valve is greater than other positions. And the maximum velocity appears at the corner of the bottom of the valve disc and valve seat, which is mainly due to the tearing and erosion of the pump valve and valve seat. This phenomenon just corresponds to the actual failure position of the pump valve and valve seat. The results of this paper can be used to verify the flow field laws of reciprocating pump hydraulic end with the same principle, and provides an effective method and theoretical basis for further studies on reciprocating pump design, valve disc and valve seat erosion failure mechanism.

Keywords: Fracturing pump; Failure; Flow field; Valve; Erosion.

1. Introduction

Shale gas reservoirs with characteristics of ultra-low permeability, low porosity and diversity of gas occurrence, generally have lower or even no production [1,2]. High-pressure reciprocating pumps are widely used in the fracturing process, and plunger pumps with small power and large power have been widely concerned and developed. Many experts and scholars have done a lot of research on reciprocating fracturing pumps [3]. Huang QY et al. [4,5] completed the design of the overall transmission scheme of 2000HP long-stroke drilling pumps and the determination of performance parameters. The structure design and strength check of the key transmission parts of the power end are carried out, and a new type of multi-pivot crankshaft is designed. The mechanical properties of the new type of crankshaft are analyzed, and the results prove the superiority of the new type of crankshaft. Arnaud L et al. [6,7] combined with fluid mechanics theory and related software, studied the interaction between heat and fluid of the parts of the reciprocating plunger pump during operation, and found that the initial fluid temperature field and the running speed of the plunger would affect the operating efficiency of the reciprocating pump, and the research results provided a theoretical basis for the operating mechanism and characteristics of the reciprocating pump. Wang Mengyi et al. [8,9] analyzed the erosion rules of gas pipelines with different structures by using fluid-structure coupling erosion method, and optimized the pipeline structure Based on the Discrete Phase Model (abbreviated as DPM). Finally, it was confirmed that the optimization of the structure was conducive to the mitigation of pipeline erosion by using comparative analysis method. Xiaotian Huang et al. [10,11] studied the erosion of the centralizer by high-speed fluid based on the Computational Fluid Dynamics (abbreviated as CFD) method, obtained the operation law of the flow field at the position of diameter reduction and shape change, as well as the solid phase erosion of the blade of the centralizer. The valve seat and valve core of the reciprocating pump were also in the position of flow channel

https://doi.org/10.17683/ijomam/issue22.v1.10

change. Therefore, this paper can make use of the previous research results on the reciprocating pump valve seat and valve body received solid phase erosion research, find the failure reasons of the valve seat and valve core, and provide theoretical basis for improving the structure of the valve seat and valve core.

Previous literature has also done a correlation analysis, but the lack of detailed and reasonable analysis process. The flow field inside the pump head is over simplified, it cannot really indicate the law of fluid flow. And there are few literature about the simulation of three-dimensional flow field. An accurate three-dimensional fluid model is established based on field data and relevant design data in this paper. The velocity change of fluid near the valve and valve seat under various transient conditions is simulated. The distribution of valve gap on valve and valve seat is analyzed to clearly understand and optimize the internal structure of the hydraulic end.

2. Five Cylinder Plunger Pump Working Principle

Five-cylinder plunger pump belongs to volume pump, the periodic change of working chamber volume is produced by reciprocating motion of plunger in the hydraulic cylinder. Fig.1 is the working principle diagram of five cylinder in a single cylinder plunger pump, Fig.1 (a) shows the crank OA rotating with uniform angular velocity of, when the crank rotating angle ＝0-π, it is the suction stroke, the crank rotating angle ＝π-2π, it is the discharge stroke. Fig. 1(b) is the diagram of rise and descending process of suction valve and discharge valve hydraulic end.

The movement of cross head and piston is the same, so the movement of B in the center of cross head pin can be indicated the movement of piston. We can see from Fig.1, plunger displacement formula.

$$s \approx r(1 \mp \cos\varphi \pm \frac{\lambda}{2}\sin^2\varphi) \tag{1}$$

Plunger velocity formula:

$$u \approx \pm r\omega(\sin\varphi + \frac{\lambda}{2}\sin^2\varphi) \tag{2}$$

The valve lift distance formula:

$$h = \frac{A_1 \omega r \sin\omega t}{\mu\pi d_1\sqrt{\frac{2(G+R)}{A_2\rho}\sin\theta}} \tag{3}$$

In the formula:

A_1—The cross sectional area of piston; A_2—Valve disc area; μ—The flow coefficient of valve, here is 1.12; ρ—Medium density; *h*—valve disc lift; ω—Crank angular velocity, *R*—spring force, 298N; θ—the angle between the surface and the valve disc with the axis.

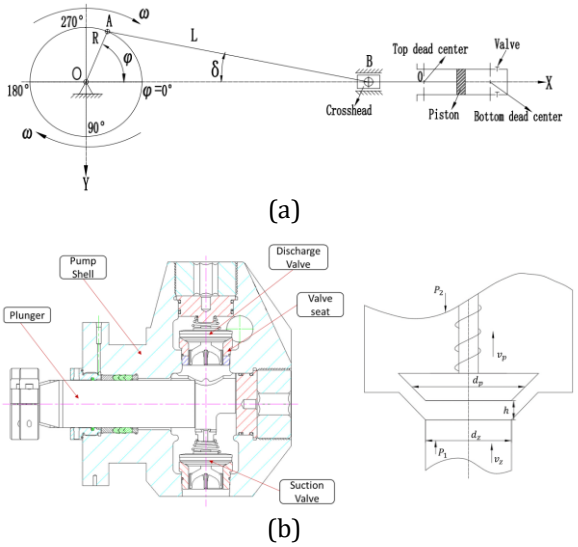

Figure 1: The working principle of plunger pump

P_1—Valve plate bottom surface pressure, MPa; P_2—Valve plate upper surface pressure, MPa; v_z—Velocity valve seat bore fluid, m/s; v_p—Valve plate rising velocity, m/s; d_z—Valve seat bore diameter, mm; d_z—Valve plate diameter, mm; *h*—Height of valve plate rising, mm.

Fracturing construction "Ten thousand cubic meters of liquid, thousand cubic meters of sand" has become the trend of future development, especially under high pressure; large displacement output has become China's "Fracturing factory" development characteristics as shown in Fig.2 and Fig.3.

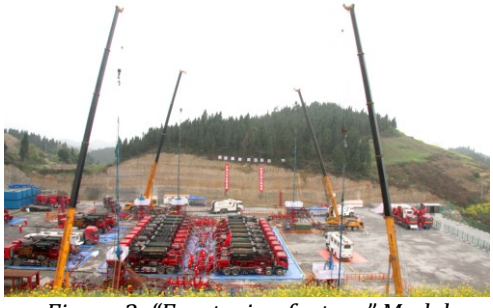

Figure 2: "Fracturing factory" Model

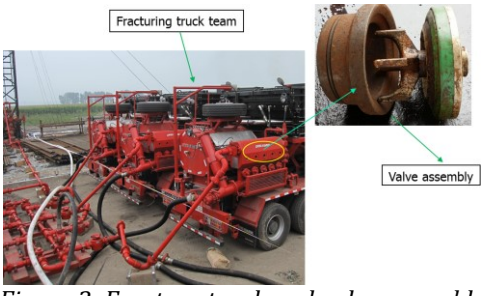

Figure 3: Fracture truck and valve assembly

For the fracturing pump, the efficiency of the pump and the frequent failure forms during operation, such as the damage of the valve body (valve core), the puncture of the pump head, the erosion of the cavity wall, and the wear failure of the valve seat, are shown in Fig.4.

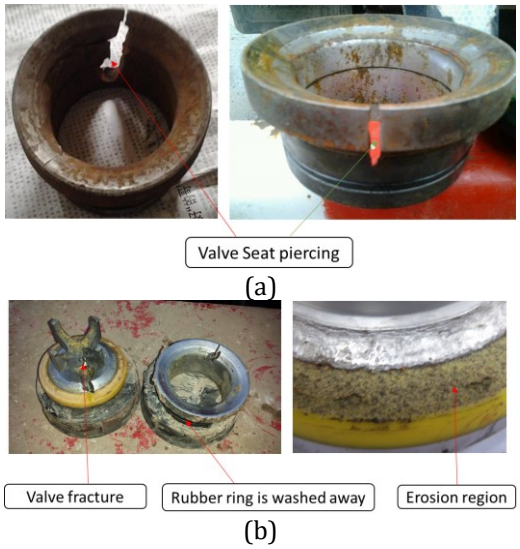

Figure 4: Failure photos of valve seat and valve disc

3. Numerical Calculation Equation

The flow of fluids is controlled by the laws of conservation of mass, momentum, and energy, if the flow is in a turbulent state, the system also follows the additional turbulent transport equation, the control equation is a mathematical description of these conservation laws, the mathematical description of the physical model of the flow problem is given, that is the basic equation of flow (control equation) and its boundary conditions are given, which is known as mathematical model. The establishment of mathematical model is based on the physical model, in the study of the hydraulic end of the plunger pump, the geometry of the internal fluid region of the hydraulic end of the plunger pump is established by a three-dimensional solid model, flow state is in turbulent flow [12,13]. Therefore, the mathematical model obtained is as follows:

1) Mass conservation equation

$$\frac{\partial \rho}{\partial t}+\frac{\partial}{\partial x}(\rho v_x)+\frac{\partial}{\partial r}(\rho v_r)+\frac{\rho v_r}{\partial r}=0 \tag{4}$$

2) Momentum conservation equation

$$\frac{\partial(\rho u_i)}{\partial t}+\frac{\partial(\rho u_i u_j)}{\partial x_i}=-\frac{\partial p}{\partial x_i}+\frac{\partial}{\partial x_i}(\eta\frac{\partial u_i}{\partial x_j}-\rho u_i' u_j') \tag{5}$$

3) Energy-balance equation

$$\frac{\partial}{\partial t}(\rho T)+\frac{\partial}{\partial x}(\rho v_x T)+\frac{\partial}{\partial y}(\rho v_r T)=\frac{\partial}{\partial x}(\frac{k}{c_p}\frac{\partial T}{\partial x})+\frac{\partial}{\partial y}(\frac{k}{c_p}\frac{\partial T}{\partial y})+S_r \tag{6}$$

Where, ρ— density of fluid, kg/m^3; v_x—Axial velocity vector, m/s; v_r—Radial velocity vector, m/s;t—Time,s; x—Axial displacement, m; r—Radial displacement, m. p—Pressure, Pa; u_i— the velocity of x direction, m/s;uj—the velocity of y direction,m/s; η_t —Turbulent viscosity coefficient,kg/ (m·s) ; x_i—the displacement of x direction, m; y_j—the displacement of y direction, m; cp—the specific heat capacity, J/ (kg·℃) ; T—Temperature; k— fluid heat transfer coefficient; S_r—viscous dissipation phase of fluid.

In order to further explore the relationship between the valve internal flow velocity and pressure distribution and movement of the plunger pump, the parameters of suction process and discharge process under seven strokes (or rotating speed) are obtained by calculating, and the parameters values are shown in Table 1, Table 2.

Table 1. Parameter values of suction process

Stroke n/rpm	Crank angle φ /°	Lift distance/ mm	velocit/ m/s)	Displace-ment/ m	Suction pressure/ MPa
79	15	0.789	0.23	4.12	0.3
	30	1.524	0.49	16.1	
	60	2.640	0.80	58.2	
	90	3.048	0.84	111.5	

Table 2. Parameter values of discharge process

Stroke n/rpm	Crank angle φ /°	Lift distance / mm	velocity/ (m/s)	Displace-ment/ m	Discharge pressure/ MPa
79	195	0.829	0.18	2.74	105
	210	1.596	0.35	11.1	
	240	2.782	0.66	43.4	
	270	3.040	0.84	91.7	

4. Calculation Results Analysis

4.1 Velocity Change Rule under Different Stroke During Working Process

It shows that the velocity vector diagram of the crank at the maximum and minimum speed shown in Fig. 5 and Fig. 6 that the larger the velocity of the fluid is concentrated in the gap area between the valve seat and the valve body. When the stroke times are 79rpm, the smaller the angle is, the smaller the rising height of the valve body is, and the fluid flow rate in the suction chamber becomes larger. When the number of strokes is 299rpm, with the increase of the rotation angle, the higher the rising height is, the greater the fluid velocity in the suction chamber becomes, and the fluid velocity in the suction chamber is also relatively large. The maximum flow rate increases with the increase of the opening, reaching 18.35m/s.

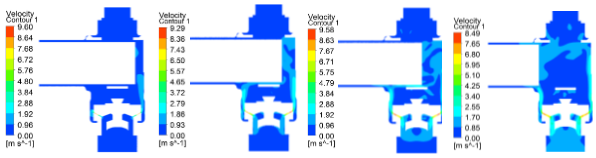

a (ø=15°) b (ø=30°) c (ø=60°) d (ø=90°)

Fig. 5 Velocity contour of suction chamber at 79 rpm under crank angle

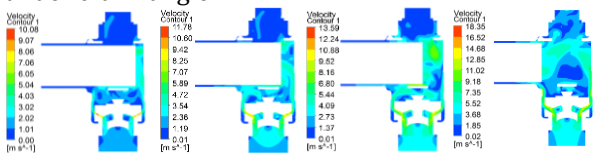

a (ø=195°) b (ø=210°) c (ø=240°) d (ø=270°)

Figure 6: Velocity contour of suction chamber at 299 rpm under crank angle

It shows the fluid velocity vector diagram at the maximum and minimum speed shown in Fig. 7 and Fig. 8 that the larger fluid velocity is also concentrated in the clearance area between the valve seat and the pump valve. Moreover, the larger the rising height of the valve body and the smaller the angle, the smaller the fluid flow in the discharge chamber. Basically, the fluid velocity changes little, and the maximum velocity does not increase with the increase of the opening. The fluid velocity basically does not change much, and the maximum velocity does not increase with the increase of the opening. When the rotation angle is ø =15°, there is a large flow rate at the gap between the valve and the valve seat, and the maximum flow rate reaches 9.23m/s. When the stroke is 299rpm, the valve body rises higher with the increase of rotation angle, and the fluid velocity in the discharge chamber is relatively high. The maximum velocity increases with the increase of opening, and the maximum velocity reaches 18.72m/s. In addition, some vortices and backflows will occur when the fluid flows through the inner chamber. Therefore, the fluid has a certain impact on the discharge chamber at the maximum stroke

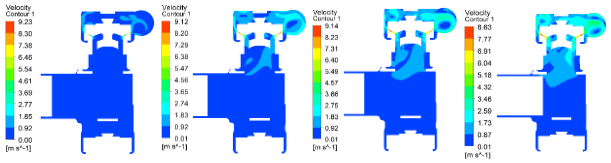

a (ø=15°) b (ø=30°) c (ø=60°) d (ø=90°)

Figure 7: Velocity contour of discharge chamber at 79 rpm under crank angle

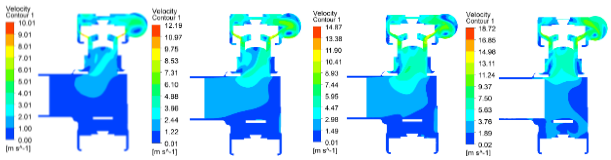

a (ø=195°) b (ø=210°) c (ø=240°) d (ø=270°)

Figure 8: Velocity contour of discharge chamber at 299 rpm under crank angle

4.2 Velocity Change under Different Stroke During the Suction Process

As shown in Fig.9, it shows that the velocity increasing gradually, the maximum speed appearance in the valve clearance, and the speed from small to large and then from small to large when the crank turns the same angle. with the rotate angle increasing, the velocity curve of hump section becomes stable, the increase of speed will slow down, especially at the 15°, the increment of velocity is the largest, when the rotate angles are 30°, 45°and 60°, the velocity change curve is similar, it slowed down relative to 15°, when the rotate angle is 75°and 90°, the increment of velocity is the smallest. It shows the change of velocity of the flow field is also relate to the opening of the valve body and the speed of the plunger in the suction process.

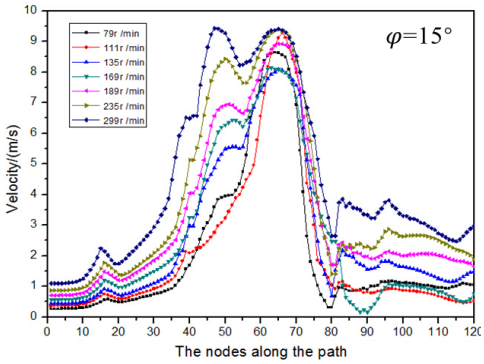

(a)

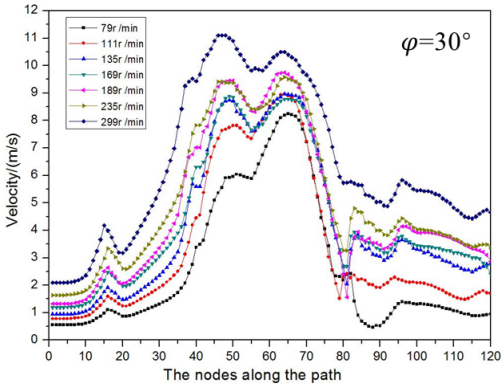

(b)

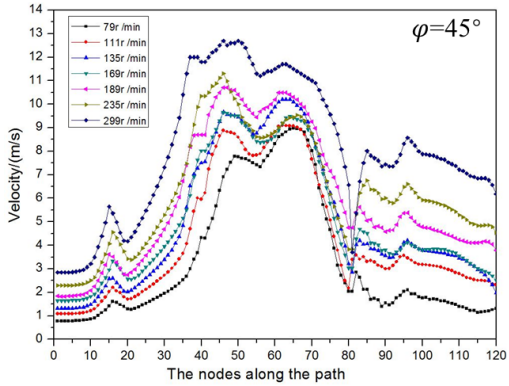

(c)

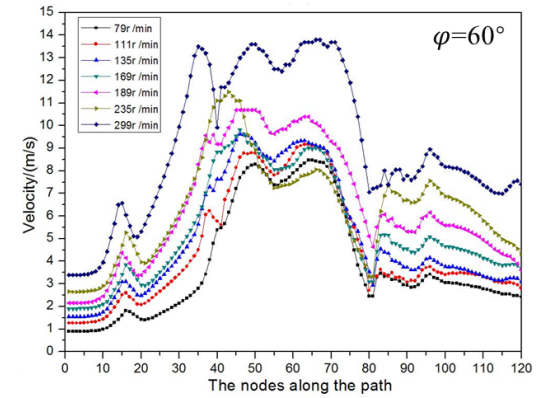

(d)

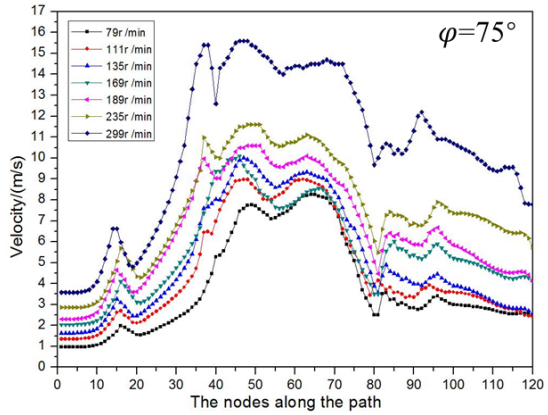

(e)

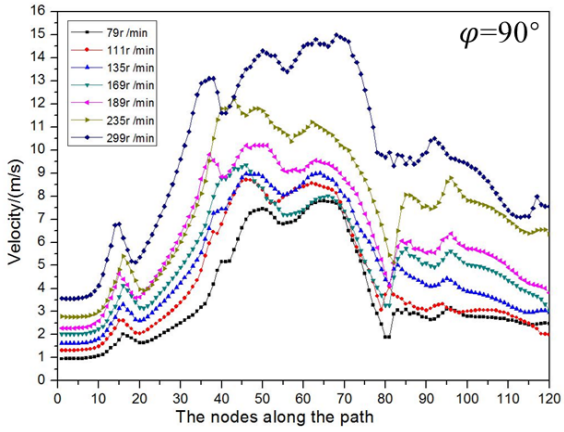

(f)

Figure 9: Velocity curve of fluid in the suction process

As shown in Fig. 10, the maximum velocity increases with the rotate angle increasing in the suction and discharge process, and then becomes small, the changes of the maximum velocity has little difference in the suction and discharge process, the curve of the maximum velocity shows a positive cosine distribution in the suction and discharge process, which is relative to the reciprocating pump, and the correctness of the velocity and displacement formula of the plunger motion is verified reasonably.

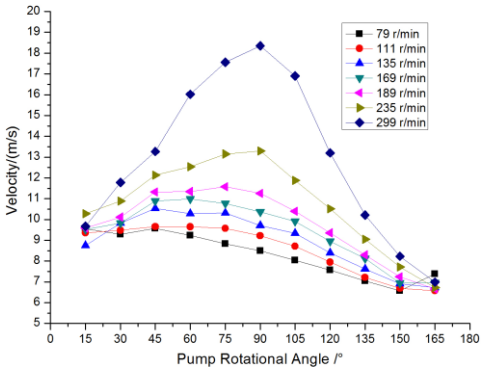

(a) 79 rpm

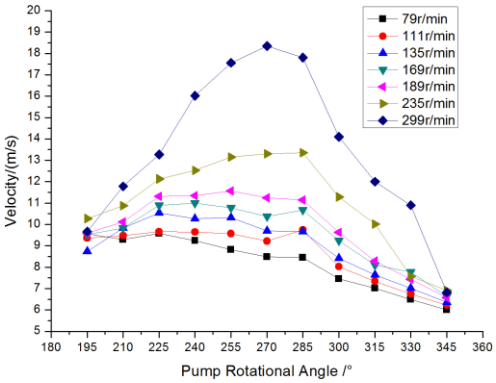

(b) 299 rpm

Figure 10: Velocity curve of fluid in the discharge chamber under 79 rpm and 299 rpm

5. Analysis of Erosion Process of Valve and Valve Seat

In this paper, based on the plastic erosion theory of FLUENT（Ansys Fluent - Fluid Simulation Software）. Simulation analysis of the valve body of the abrasive erosion has been done [14-17], and the erosion rate is defined as：

$$R_{erosion} = \sum_{p=1}^{N_{particles}} \frac{m_p C(d_p) f(\alpha) v^{b(v)}}{A_{face}} \quad (7)$$

Where $C(d_p)$ is the function of particle diameter, α is the impact angle of particle on Wall, $f(\alpha)$ is the function of incidence angle, υ is the particle velocity relative to the wall surface, $b(\upsilon)$ is the relative velocity function. According to the experimental study of Ahlert, the expression model of erosion rate：

$$ER = AF_S V^n f(\alpha) \quad (8)$$

$$C(d_p) = 1.559 B^{-0.59} \times 10^{-7} \quad (9)$$

$$C(d_p) = AF_s \quad (10)$$

Where F_S is the particle shape factor F_S is 1.0 that indicates the particles with sharp angles, 0.5 indicates Half round particle, 0.2 that indicates Spherical particles; B is Bush hardness; $f(\alpha)$ is the incident angle function, the expression is as follows and the related parameter is as shown in Table.3:

$$f(\alpha)=\begin{cases} a_1\alpha^2+b_1\alpha & \alpha \le 0.262 \\ x_1\cos^2\alpha\sin\alpha+y_1\sin^2\alpha+z_1 & \alpha > 0.262 \end{cases} \quad (11)$$

Table 3. The related parameter

a_1	b_1	x_1	y_1	z_1
0.384	0.227	0.03147	0.003309	0.02532

According to the plastic erosion theory of FLUENT, we only select two representative cases in this paper, when the strokes are 79rpm and 299rpm and the crankshaft angle is 90°and 270°respectively, the results of erosion wear simulation are obtained, as shown in the following Fig.13- Fig.16.

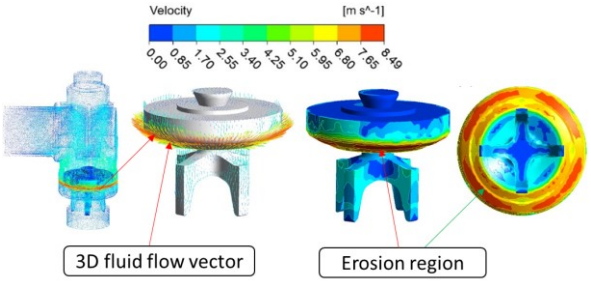

Figure 11: Erosion images under 79rpm of stroke and 90°of rotate angle

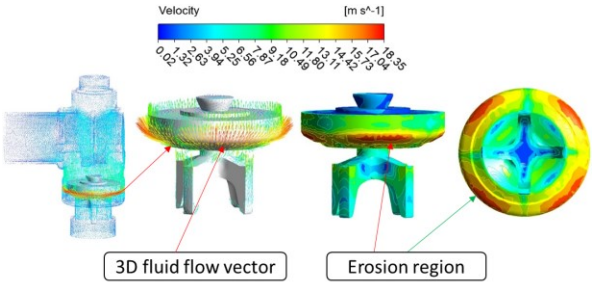

Figure 12: Erosion images under 299rpm of stroke and 90°of rotate angle

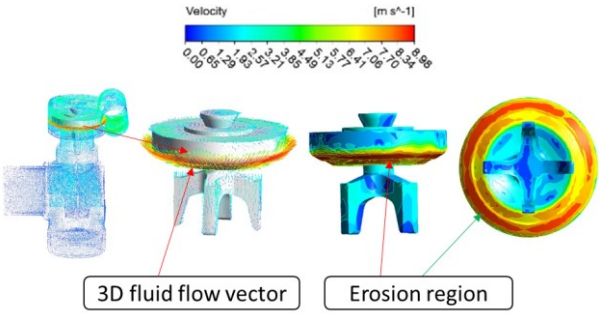

Figure 13: Erosion images under 79rpm of stroke and 270°of rotate angle

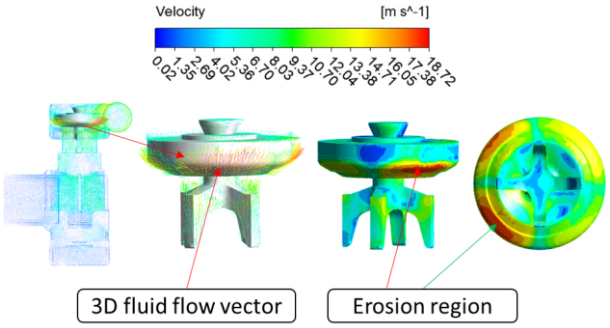

Figure 14: Erosion images under 299rpm of stroke and 270°of rotate angle

Combined with the simulation analysis and the actual image data as shown in Fig.15, analysis of the particle erosion showed that, the position of the rubber sleeve connect with the bottom surface of the valve body is the most severe erosion area, then the region of valve disc and valve seat cone surface fitting, once the cone surface is worn serious, which will bring about the seal failure of valve rubber ring. At the same time, during the working process of plunger pump, a high-speed liquid will generate in the internal of hydraulic end, which will lead to erosion failure of valve disc and valve seat, it can effectively evaluate the life and the wear rate of valve disc and valve seat assessing through these researches.

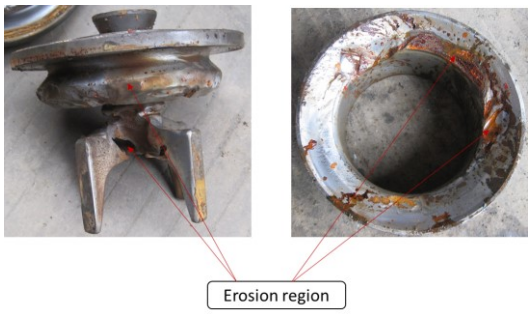

Figure 15: Erosion region of the valve disk and valve seat

Through theoretical research, simulation calculation, the actual situation contrast analysis, and speed mutation will appear in the case of a small stroke and rotate angle, such as the rotate angle is 15°or 195°and the stroke is 79rpm, at this time the velocity is larger than a bigger stroke and rotate angle. So similarly, whether in the course of discharging or suctioning, the fluid will also erode the valve disc and valve seat under a small stroke and rotate angle.

6. Conclusions

In both the suction and discharge stages, the maximum velocity of the fluid increases with the increase of the angle of rotation and then decreases gradually. There is little difference between the

maximum velocity in the suction process and the discharge process.

As the angle is small and the gap between the valve body and the valve seat is small, the cross-sectional area of the outlet becomes smaller, and the fluid velocity will have a local sudden change, resulting in a huge erosion of the hole and the wall surface in contact with the fluid.

The changes of the maximum velocity have little difference, the velocity of fluid flow shows a positive cosine distribution in the suction and discharge process, and the correctness of the velocity and displacement formula of the plunger motion is verified reasonably.

The particle erosion wear analysis of the valve body shows that the most serious erosion area of the valve body is the lower bottom surface of the valve body rubber sleeve connected with the valve body, followed by the mating cone.

The impact times of the pump are the most important factors affecting the erosion wear of the pump valve. Therefore, optimizing the impact times of the pump can significantly improve the wear of components at the hydraulic end.

References

[1] Liu Yang, Qian Liqin, Xia Chengyu, et al. Design and experimental study on a novel sealing structure of rotary control head for coalbed methane underbalanced drilling[J]. Engineering Failure Analysis139(2022)106441. https://doi.org/10.1016/j.engfailanal.2022.106441

[2] Liu Yang, Lian Zhanghua. Failure analysis on rubber sealing structure of mandrel hanger and improvement in extreme environments. [J]. Engineering Failure Analysis 125 (2021) 105433.https://doi.org/10.1016/j.engfailanal.2021.105433

[3] Huang Qiyue，Hou Yongjun，Xi Jianqiu. Dynamic characteristics analysis of long stroke reciprocating pump combined crank-linkage with rack-pinion mechanism[J].Proceedings of Institution of Mechanical Engineers Part C Journal of Mechanical Engineering Science 237(17) (2023) 3850-3860. https://doi.org/10.1177/09544062221148877

[4] Feng Jianmei, Zhang Qingqing, Hou Tianfang, et al. Dynamics characteristics analysis of the oil-free scroll hydrogen recirculating pump based on multibody dynamics simulation[J]. International Journal of Hydrogen Energy46(7) (2020)5699-5713.https://doi.org/10.1016/j.ijhydene.2020.11.065

[5] Wang Hang, Yang Shangyu, Han Lihong, et al. Failure analysis of crankshaft of fracturing pump[J]. Engineering Failure Analysis109(2020)104378. https://doi.org/10.1016/j.engfailanal.2020.104378

[6] Arnaud L, Nicolas T, Rémi R, et al. Performance investigation of reciprocating pump running with organic fluid for organic Rankine cycle[J]. Applied Thermal Engineering113(2017)962-969. https://doi.org/10.1016/j.applthermaleng.2016.11.096

[7] Zhu Hongjun, Gao Yue, Srinil N,et al. Mode switching and standing-travelling waves in slug flow-induced vibration of catenary riser[J]. Journal of Petroleum Science and Engineering203(2021) 108310.https://doi.org/10.1016/j.petrol.2020.108310

[8] Wang Mengyi, Chen Yan, Liu Yang,et al. Analysis and Optimization of Fluid Solid Coupling Erosion in Gas Pipeline Based on DPM Model[J]. Journal of Failure Analysis and Prevention23 (04)(2023)1701-1714. https://doi.org/10.1007/s11668-023-01716-6.

[9] Bahareh Nemati, Mohammad Vaghefi, Mahdi Behroozi. Numerical investigation of the erosion reduction in elbows using separate and helical inner ring [J]. Results in Engineering 23(2024)102499.https://doi.org/10.1016/j.rineng.2024.102499.

[10] Huang Xiaotian,Chen Yan,Fan Junqiang. Research on Erosion and Wear Law of Stabilizer Blade based on CFD-DPM Model[J].International Journal of Mechatronics and Applied Mechanics18(2024)190-198. https://doi.org/10.17683/ijomam/issue18.23

[11] Parkash Om, kumar Arvind, Sikarwar Basant Singh, et al. CFD modeling of slurry flow erosion wear rate through mitre-pipe bend[J]. Proceedings of the Institution of Mechanical Engineers, Part C: Journal of Mechanical Engineering Science, 236(5) (2022)2256-2267. https://doi.org/10.1177/09544062211026353

[12] Tomasz Szwarc, Włodzimierz Wróblewski, Tomasz Borzęcki. Optimization of the Aircraft Air/Oil Separator by the Response Surface Determined from Modeling of Three-Dimensional Two-Phase Flow[J]. Energies15(2022) 7273. https://doi.org/10.3390/en15197273

[13] Meng Yu, Quan Shenglin, Guo Yali,et al. Comparative Analysis of Dynamic Behavior of Liquid Droplet Impacting Flat and Circular

Wires[J]. Energies15 (2022) 6623. https://doi.org/10.3390/en15186623

[14] Swaleha Kazi, Sudhakar Umale, M. Venkatesh, et al. Application of various correlations for design of demisters to study the effect of geometrical parameters on its performance[J]. Materials Today: Proceedings38(5)(2021)3035-3040. https://doi.org/10.1016/j.matpr.2020.09.381

[15] Nuri Elsheikh, Amir H. Azimi, Ioan Nistor, et al. Tsunami-Induced Bores Propagating over a Canal, Part II: Numerical Experiments Using the Standard k-ε Turbulence Model[J]. Fluids7(7)(2022) 214. https://doi.org/10.3390/fluids7070214

[16] M. Nur Alam Zico, Md. Aliur Rahman, Hazzaz Bin Yusuf, et al. CFD modeling of drill cuttings transport efficiency in annular bends: Effect of hole eccentricity and rotation[J]. Geoenergy Science and Engineering 221(2023) 211380. https://doi.org/10.1016/j.geoen.2022.211380

[17] Pang Boxue, Wang Shuyan, Lu Cailei, et al. Investigation of cuttings transport in directional and horizontal drilling wellbores injected with pulsed drilling fluid using CFD approach[J]. Tunnelling and Underground Space Technology 90 (2019) 183–193. https://doi.org/10.1016/j.tust.2019.05.001